

February 26, 2024

Improved measurements of D_s meson decay constant and branching fractions of $D_s^+ \rightarrow K^- K^+ \pi^+$, $\bar{K}^0 K^+$ and $\eta \pi^+$ decays from Belle

ANŽE ZUPANC

FOR THE BELLE COLLABORATION

*Karlsruher Institut für Technologie**Institut für Experimentelle Kernphysik, 76131 Karlsruhe, Germany*

We present preliminary absolute branching fraction measurements of leptonic D_s^+ decays to $\mu^+ \nu_\mu$ and $\tau^+ \nu_\tau$, and of hadronic D_s^+ decays to $K^- K^+ \pi^+$, $\bar{K}^0 K^+$ and $\eta \pi^+$. The results are obtained from a large data sample collected near the $\Upsilon(4S)$ and $\Upsilon(5S)$ resonances with the Belle detector at the KEKB asymmetric-energy $e^+ e^-$ collider. We obtain the the branching fractions $\mathcal{B}(D_s^+ \rightarrow \mu^+ \nu_\mu) = (0.528 \pm 0.028 \pm 0.019)\%$ and $\mathcal{B}(D_s^+ \rightarrow \tau^+ \nu_\tau) = (5.70 \pm 0.21_{-0.30}^{+0.31})\%$ which are combined to determine the D_s decay constant $f_{D_s} = (255.0 \pm 4.2 \pm 5.0)$ MeV, where the first and second uncertainties are statistical and systematic, respectively. Branching fractions of hadronic decays are measured to be $\mathcal{B}(D_s^+ \rightarrow K^- K^+ \pi^+) = (5.06 \pm 0.15 \pm 0.19)\%$, $\mathcal{B}(D_s^+ \rightarrow \bar{K}^0 K^+) = (2.84 \pm 0.12 \pm 0.08)\%$ and $\mathcal{B}(D_s^+ \rightarrow \eta \pi^+) = (1.79 \pm 0.14 \pm 0.05)\%$.

PRESENTED AT

The 5th International Workshop on Charm Physics
Honolulu, Hawai'i, USA, May 14–17, 2012

1 Introduction

The leptonic decays of mesons provide access to experimentally clean measurements of the meson decay constants or the relevant Cabibbo-Kobayashi-Maskawa matrix elements. In the Standard Model (SM) the branching fraction for a leptonic decay of a charged pseudoscalar meson, such as D_s^+ , is given by [1, 2]:

$$\mathcal{B}(D_s^+ \rightarrow \ell^+ \nu_\ell) = \frac{\tau_{D_s} M_{D_s}}{8\pi} f_{D_s}^2 G_F^2 |V_{cs}|^2 m_\ell^2 \left(1 - \frac{m_\ell^2}{M_{D_s}^2}\right)^2, \quad (1)$$

where M_{D_s} is the D_s mass, τ_{D_s} is its lifetime, m_ℓ is the lepton mass, V_{cs} is the Cabibbo-Kobayashi-Maskawa (CKM) matrix element between the D_s constituent quarks c and s , and G_F is the Fermi coupling constant. The parameter f_{D_s} is the decay constant, and is related to the wave-function overlap of the quark and anti-quark. The leptonic decays of pseudoscalar mesons are suppressed by helicity conservation and their decay rates are thus proportional to the square of the lepton mass. Leptonic D_s decays into electrons are not observable whereas decays to taus are favored over decays to muons in spite of the reduced phase-space in the former case.

If the magnitude of the relevant CKM matrix element is well known from other measurements then by measuring the leptonic branching fraction of a pseudoscalar meson one can determine the decay constant with high precision. Conversely, if one can precisely estimate the decay constant of a pseudoscalar meson, it is possible to determine the magnitude of the relevant CKM element.

Measurements of f_{D_s} have been made by several groups: CLEO-c [3, 4, 5], Belle [6] and BaBar [7]. Rosner and Stone combined the above measurements and report the experimental world average to be $f_{D_s}^{\text{exp}} = (260 \pm 5.4) \text{ MeV}$ [2]. Within the SM, f_{D_s} has been predicted using several methods [8, 9, 10, 11, 12, 13, 14]. While most calculations give values lower than the f_{D_s} measurement, the errors on predicted values are too large in most cases to claim any disagreement with experiment. The largest discrepancy (2.0 standard deviations) is with an unquenched lattice QCD (LQCD) calculation: $f_{D_s}^{\text{LQCD}} = (248 \pm 2.5) \text{ MeV}$ [8]. There are several theoretical scenarios in which non SM particles may modify the leptonic decay rates of the D_s meson. Akeroyd and Chen pointed out that leptonic decay widths are modified in two-Higgs-doublet models (2HDM) [15]. Measurements of f_{D_s} with an accuracy that matches the precision of theoretical calculations are thus necessary in order to discover or constrain effects of NP.

In these proceedings we present preliminary results of absolute branching fraction measurements of $D_s^+ \rightarrow \mu^+ \nu_\mu$ and $D_s^+ \rightarrow \tau^+ \nu_\tau$ decays* which supersede the previous measurement of $\mathcal{B}(D_s^+ \rightarrow \mu^+ \nu_\mu)$ by Belle [6] performed on a smaller data sample. This analysis is based on a data sample of 913 fb^{-1} recorded near $\sqrt{s} = 10.68 \text{ GeV}$ by the Belle detector at the KEKB asymmetric-energy collider [16].

*Charge conjugation is assumed throughout this note unless stated otherwise.

2 Belle detector

The Belle detector is a large-solid-angle magnetic spectrometer that consists of a silicon vertex detector (SVD), a 50-layer central drift chamber (CDC), an array of aerogel threshold Cherenkov counters (ACC), a barrel-like arrangement of time-of-flight scintillation counters (TOF), and an electromagnetic calorimeter (ECL) comprised of CsI(Tl) crystals located inside a superconducting solenoid coil that provides a 1.5 T magnetic field. An iron flux-return located outside of the coil is instrumented to detect K_L^0 mesons and to identify muons (KLM). The detector is described in detail elsewhere [17]. Two inner detector configurations were used. A 2.0 cm beampipe and a 3-layer silicon vertex detector was used for the first sample of 156 fb^{-1} , while a 1.5 cm beampipe, a 4-layer silicon detector and a small-cell inner drift chamber were used to record the remaining 757 fb^{-1} of data.

Tracks are detected with the CDC and the SVD. They are required to have an impact parameter with respect to the interaction point of less than 0.5 cm in the radial direction and less than 1.5 cm in the beam direction. A likelihood ratio for a given track to be a kaon or pion, $\mathcal{L}_{(K,\pi)}$, is obtained by utilizing specific ionization energy loss measurements in the CDC, light yield measurements from the ACC, and time-of-flight information from the TOF. For electron identification we use position, cluster energy, shower shape in the ECL, combined with track momentum and dE/dx measurements in the CDC and hits in the ACC. For muon identification, we extrapolate the CDC track to the KLM and compare the measured range and transverse deviation in the KLM with the expected values. Photons are required to have energies in the laboratory frame of at least 50 - 100 MeV, depending on the detecting part of the ECL. Neutral pion candidates are reconstructed using photon pairs with invariant mass between 120 and 150 MeV[†]. Neutral kaon candidates are reconstructed using charged pion pairs with invariant mass within ± 20 MeV of the nominal K^0 mass.

3 Overview of the method

The method of absolute branching fraction measurement of $D_s^- \rightarrow \ell^- \bar{\nu}_\ell$ decays is similar to the one previously used by the Belle collaboration [6] and more recently by the Babar collaboration [7]. In this method the $e^+e^- \rightarrow c\bar{c}$ events which contain D_s^- mesons produced through the following reactions:

$$e^+e^- \rightarrow c\bar{c} \rightarrow D_{\text{tag}} K X_{\text{frag}} D_s^{*-}, D_s^{*-} \rightarrow D_s^- \gamma, \quad (2)$$

are fully reconstructed in two steps. In these events one of the two charm quarks hadronizes into a D_s^{*-} meson while the other quark hadronizes into a charm hadron denoted as D_{tag} (tagging charm hadron). We reconstruct the tagging charm hadron

[†]We use natural units throughout this note.

as D^0 , D^+ , $\Lambda_c^{+\dagger}$, D^{*+} or D^{*0} . The strangeness of the event is conserved by requiring additional kaon, denoted as K , which can be either K^+ or K_S^0 . Since Belle collected data at energies well above $D_{\text{tag}}^{(*)}KD_s^*$ threshold additional particles can be produced in the process of hadronization. These particles are denoted as X_{frag} and can be: even number of kaons and or any number of pions or photons. In this measurement only pions are considered when reconstructing the fragmentation system X_{frag} . We require D_s^- mesons to be produced in a $D_s^{*-} \rightarrow D_s^- \gamma$ decay which provides powerful kinematic constraint (D_s^* mass, or mass difference between D_s^* and D_s) that improves the resolution of the missing mass (defined below) and suppresses the combinatorial background.

In the first step of the measurement no requirements are placed on the daughters of the signal D_s^- meson in order to obtain a fully inclusive sample of D_s^- events which is used for normalization in the calculation of the branching fractions. The number of inclusively reconstructed D_s mesons is extracted from the distribution of events in the missing mass, $M_{\text{miss}}(D_{\text{tag}}KX_{\text{frag}}\gamma)$, recoiling against the $D_{\text{tag}}KX_{\text{frag}}\gamma$ system:

$$M_{\text{miss}}(D_{\text{tag}}KX_{\text{frag}}\gamma) = \sqrt{p_{\text{miss}}(D_{\text{tag}}KX_{\text{frag}}\gamma)^2}, \quad (3)$$

where p_{miss} is the missing momentum in the event:

$$p_{\text{miss}}(D_{\text{tag}}KX_{\text{frag}}\gamma) = p_{e^+} + p_{e^-} - p_{D_{\text{tag}}} - p_K - p_{X_{\text{frag}}} - p_\gamma. \quad (4)$$

Here, p_{e^+} and p_{e^-} are the momenta of the colliding positron and electron beams, respectively, and the $p_{D_{\text{tag}}}$, p_K , $p_{X_{\text{frag}}}$, and p_γ are the measured momenta of the reconstructed D_{tag} , kaon, fragmentation system and the photon from $D_s^* \rightarrow D_s \gamma$ decay, respectively. Correctly reconstructed events given in the Eq. 2 produce a peak in the $M_{\text{miss}}(D_{\text{tag}}KX_{\text{frag}}\gamma)$ at nominal D_s meson mass.

In the second step we search for the purely leptonic $D_s^+ \rightarrow \mu^+ \nu_\mu$ and $D_s^+ \rightarrow \tau^+ \nu_\tau$ decays within the inclusive D_s^+ sample by requiring an additional charged track identified as an electron, muon or charged pion to be present in the rest of the event. In case of $D_s^+ \rightarrow \tau^+ \nu_\tau$ decays the electron, muon or charged pion track identifies the subsequent τ^+ decay to $e^+ \nu_e \bar{\nu}_\tau$, $\mu^+ \nu_\mu \bar{\nu}_\tau$ or $\pi^+ \bar{\nu}_\tau$. Hadronic decays, $D_s^+ \rightarrow \bar{K}^0 K^+$ and $\eta \pi^+$, are reconstructed partially by only requiring that an additional charged kaon or pion is present in the rest of the event while no requirements are set upon the neutral hadrons (\bar{K}^0 or η) in order to increase the reconstruction efficiency. In case of $D_s^+ \rightarrow K^- K^+ \pi^+$ all three charged tracks are required to be present in the rest of the event.

[†]In events where Λ_c^+ is reconstructed as tagging charm hadron additional \bar{p} is reconstructed in order to conserve the total baryon number.

| $D^0 \rightarrow$ | $\mathcal{B} [\%]$ | $D^+ \rightarrow$ | $\mathcal{B} [\%]$ | $\Lambda_c^+ \rightarrow$ | $\mathcal{B} [\%]$ |
|-------------------------------|--------------------|---------------------------|--------------------|-----------------------------|--------------------|
| $K^- \pi^+$ | 3.9 | $K^- \pi^+ \pi^+$ | 9.4 | $p K^- \pi^+$ | 5.0 |
| $K^- \pi^+ \pi^0$ | 13.9 | $K^- \pi^+ \pi^+ \pi^0$ | 6.1 | $p K^- \pi^+ \pi^0$ | 3.4 |
| $K^- \pi^+ \pi^+ \pi^-$ | 8.1 | $K_S^0 \pi^+$ | 1.5 | $p K_S^0$ | 1.1 |
| $K^- \pi^+ \pi^+ \pi^- \pi^0$ | 4.2 | $K_S^0 \pi^+ \pi^0$ | 6.9 | $\Lambda \pi^+$ | 1.1 |
| $K_S^0 \pi^+ \pi^-$ | 2.9 | $K_S^0 \pi^+ \pi^+ \pi^-$ | 3.1 | $\Lambda \pi^+ \pi^0$ | 3.6 |
| $K_S^0 \pi^+ \pi^- \pi^0$ | 5.4 | $K^+ K^- \pi^+$ | 1.0 | $\Lambda \pi^+ \pi^+ \pi^-$ | 2.6 |
| Sum | 38.4 | Sum | 28.0 | Sum | 16.8 |

Table 1: Summary of $D_{\text{tag}} = D^0$, D^+ and Λ_c^+ decay modes used in this measurement. The branching fractions are taken from [1].

4 Inclusive D_s reconstruction

The reconstruction of the inclusive D_s sample starts with the reconstruction of the tagging charmed hadrons, D_{tag} . In order to increase the reconstruction efficiency of studied events, the D_{tag} is reconstructed in as many decay modes as possible, while keeping the purity of the sample at reasonable level. The ground state D_{tag} (D^0 , D^+ , Λ_c^+) hadrons are reconstructed in total in 18 hadronic decay modes (see Table 1). Only modes with up to one π^0 in the final state are used in order to avoid large backgrounds.

The center of mass momentum of the D_{tag} candidates (p^*) is required to be greater than 2.3 (or 2.5 for less clean D_{tag} modes) GeV/ c in order to reduce the background and to remove charmed hadrons originating from B decays. The decay products of the D_{tag} candidates are fitted to a common vertex and candidates with poor fit quality are discarded ($\chi^2/n.d.f < 20$). The purity of D_{tag} sample at this stage is rather low - around 17% in the signal region defined as $\pm 3\sigma$ interval around the nominal D_{tag} mass, where σ is the D_{tag} decay mode dependent invariant mass resolution. In order to further clean up the D_{tag} sample we train an NeuroBayes [19] neural network using small sample of real data (around 1% of the total sample). Network combines information from the following input variables into one single scalar output variable: the distance between the decay and the production vertices of D_{tag} candidates in $r - \phi$ plane, the $\chi^2/n.d.f$ of the vertex fit of D_{tag} candidates, the cosine of the angle between the D_{tag} momentum vector and the vector joining its decay and production vertices in $r - \phi$ plane, the cosine of the angle between the momentum of one of the D_{tag} daughters momentum vector in the D_{tag} rest frame and the D_{tag} momentum in the laboratory frame (only for two-body D_{tag} decays), particle identification likelihood ratios and for the D_{tag} decay modes including π^0 the minimal energy of the two photons. To obtain the signal and background distributions of variables entering the NeuroBayes network a statistical tool to unfold the data distributions (sPlot) is applied [20]. The cut on the network output variable is optimized for each D_{tag} mode individually by maximizing $S/\sqrt{S+B}$, where S (B) refers to the signal (background) yield in the signal window of D_{tag} invariant mass determined by performing a fit to the D_{tag} invariant mass distribution. After the optimization the purity of the correctly

reconstructed D_{tag} candidates increases from 17% to 42% while losing only around 16% of signal D_{tag} candidates. We keep only D_{tag} candidates from signal region in D_{tag} invariant mass in rest of the analysis.

Once the ground state D_{tag} hadrons have been reconstructed, D^0 and D^+ mesons originating from D^* decays are identified by reconstructing the decays $D^{*+} \rightarrow D^0\pi^+$, $D^+\pi^0$ and $D^{*0} \rightarrow D^0\pi^0$, $D^0\gamma$. The motivation for this reconstruction is to clean up the subsequent $KX_{\text{frag}}\gamma$ reconstruction; by absorbing one more particle to the tagging charm hadron the subsequent combinatoric background can be reduced. In addition, by reconstructing $D^{*+} \rightarrow D^0\pi^+$ decays we can determine of the charm quantum number of D^0 decays including neutral kaons. The slow pions from D^* decay are refitted to a D production vertex in order to improve the resolution of the mass difference, $\Delta M = M(D\pi) - M(D)$. The photon energy in the laboratory frame is required to be larger than 50 MeV for $\pi^0 \rightarrow \gamma\gamma$ and 175 MeV for $D^{*0} \rightarrow D^0\gamma$ decays. In the latter decays the γ candidate is combined with any other photon in a event, and if there exist a combination of two photons with invariant mass within 10 MeV/ c^2 around the nominal π^0 mass and their energy asymmetry $((E_{\gamma_1} - E_{\gamma_2})/(E_{\gamma_1} + E_{\gamma_2}))$ is smaller than 0.5 the D^{*0} candidate is rejected. For all D^* decays, the mass difference $m(D^*) - m(D)$ is required to be within 3σ of the corresponding nominal mass difference.

A K candidate is selected to be either K^\pm or K_S^0 candidates and does not overlap with the D_{tag} candidate.

From the remaining tracks and π^0 candidates in the event that do not overlap with the $D_{\text{tag}}K$ candidate we form X_{frag} candidates. Only modes with up to three pions and up to one π^0 are used in order to avoid large combinatoric background. In addition pions must have momentum larger than 100 MeV/ c in the laboratory frame. At this stage no requirement is applied to the total charge of the X_{frag} system.

The D_{tag} , X_{frag} and K candidates are combined to form a $D_{\text{tag}}KX_{\text{frag}}$ combinations and we keep only those with total charge ± 1 . The charm and strange quark content of the $D_{\text{tag}}KX_{\text{frag}}$ system is required to be consistent with that recoiling from a D_s^* : if D_{tag} is reconstructed in flavor specific decay mode and the primary kaon candidate is charged it is required that the kaon charge and the charm quantum number of D_{tag} are opposite to the D_s^* charge; if primary kaon candidate is a K_S^0 the charm quantum number of D_{tag} is required to be opposite to the D_s^* charge; and if D_{tag} is reconstructed in a self-conjugated decay mode the charge of the primary kaon is required to be opposite to the D_s^* charge. A kinematic fit to $D_{\text{tag}}KX_{\text{frag}}$ candidate is performed in which the particles are required to originate from a common point inside the IP region, and the D_{tag} mass is constrained to the nominal value. We select only one $D_{\text{tag}}KX_{\text{frag}}$ candidate in an event which has missing mass, $M_{\text{miss}}(D_{\text{tag}}KX_{\text{frag}}) = \sqrt{|p_{e^+} + p_{e^-} - p_{D_{\text{tag}}} - p_K - p_{X_{\text{frag}}}|^2}$, is closest to the nominal D_s^* mass and within $2.00 \text{ GeV}/c^2 < M_{\text{miss}}(D_{\text{tag}}KX_{\text{frag}}) < 2.25 \text{ GeV}/c^2$ interval (corresponding to around

$\pm 3\sigma$ interval).

Finally, a photon candidate is identified which is consistent with the decay $D_s^* \rightarrow D_s \gamma$ and does not overlap with the $D_{\text{tag}} K X_{\text{frag}}$ system. We require that the energy of the photon candidate is larger than 120 MeV in the laboratory frame and that the cosine of the angle between the direction of D_{tag} hadron and the direction of the photon candidate is negative, since the signal photon should be in opposite hemisphere of the event with respect to the D_{tag} . We perform similar kinematic fit with the signal photon included and with the missing mass recoiling against the $D_{\text{tag}} K X_{\text{frag}}$ constrained to the nominal D_s^* mass. All $D_{\text{tag}} K X_{\text{frag}} \gamma$ candidates are required to have $p_{\text{miss}}^*(D_{\text{tag}} K X_{\text{frag}} \gamma) > 2.8 \text{ GeV}/c$ and $M_{\text{miss}}(D_{\text{tag}} K X_{\text{frag}} \gamma) > 1.83 \text{ GeV}/c^2$ (see Eqs. 4 and 3). After the final selections, there are in average 2.1 $D_{\text{tag}} K X_{\text{frag}} \gamma$ candidates per event which are solely due to multiple γ candidates. We select a best $D_{\text{tag}} K X_{\text{frag}} \gamma$ candidate to be the one with the highest NeuroBayes network output which is trained to separate signal photons from photons produced in other decays. A relative gain of around 23% in absolute reconstruction efficiency is obtained by applying the best $D_{\text{tag}} K X_{\text{frag}} \gamma$ candidate selection instead of completely random selection. Figure 1 shows the distribution of $M_{\text{miss}}(D_{\text{tag}} K X_{\text{frag}} \gamma)$ for each X_{frag} mode separately.

4.1 Inclusive D_s yield extraction

The yield of inclusively reconstructed D_s mesons is determined by performing a fit to the missing mass $M_{\text{miss}}(D_{\text{tag}} K X_{\text{frag}} \gamma)$ distribution for each X_{frag} mode individually. The components of the fit are divided into six categories: signal, mis-reconstructed signal event (K candidate or one of the pions forming X_{frag} system candidate originate from D_s decay), $D^{*0} \rightarrow D^0 \gamma$ (signal γ candidate originates from D^{*0} decay), $D_{(s)}^* \rightarrow D_{(s)} \pi^0$ (one of the photons from π^0 decay from $D_{(s)}^* \rightarrow D_{(s)} \pi^0$ decay is taken to be signal γ candidate), wrong γ (the energy deposited in the ECL was produced by unmatched charged track or by beam induced interactions), and γ from π^0 (signal photon originates from a π^0 decay which does not originate from $D_{(s)}^*$ decay). Each of the above six components is parameterized with a non-parametric histogram probability density function (PDF), $\mathcal{H}(M_{\text{miss}}(D_{\text{tag}} K X_{\text{frag}} \gamma))$, taken from a large sample of Monte Carlo (MC) simulated events. The total PDF for given X_{frag} mode is thus given by:

$$\begin{aligned} \mathcal{F}^{X_{\text{frag}}}(M_{\text{miss}}(D_{\text{tag}} K X_{\text{frag}} \gamma)) &= N_{\text{sig}} \mathcal{H}_{\text{sig}}^{X_{\text{frag}}}(M_{\text{miss}}(D_{\text{tag}} K X_{\text{frag}} \gamma)) \otimes \mathcal{G}(\sigma_{\text{cal}}) \\ &+ \sum_{i=1}^5 N_{i-\text{bkg}}^{X_{\text{frag}}} \mathcal{H}_{i-\text{bkg}}^{X_{\text{frag}}}(M_{\text{miss}}(D_{\text{tag}} K X_{\text{frag}} \gamma)), \end{aligned} \quad (5)$$

where N represents the yield of each component and first (second) term in the equation describes contribution of signal (sum of five background components). Histogram PDF of signal, $\mathcal{H}_{\text{sig}}^{X_{\text{frag}}}(M_{\text{miss}}(D_{\text{tag}} K X_{\text{frag}} \gamma))$, is additionally numerically convolved

with a Gaussian function, $\mathcal{G}(\sigma_{\text{cal}})$ – centered at zero and with width σ_{cal} , which takes into account possible differences between $M_{\text{miss}}(D_{\text{tag}}KX_{\text{frag}}\gamma)$ resolutions obtained on real data and simulated samples.

The real data resolution in $M_{\text{miss}}(D_{\text{tag}}KX_{\text{frag}}\gamma)$ for signal candidates is calibrated using the mass difference between D_s^* and D_s , $\Delta M = M_{D_s^*} - M_{D_s}$, for exclusively reconstructed $D_s^* \rightarrow D_s\gamma$ decays, where D_s decays to $\phi\pi$ and $\phi \rightarrow K^+K^-$. In the exclusive reconstruction of D_s^* mesons the same requirements are used for the signal photon candidate as in the inclusive reconstruction. The dominant contribution to the resolution of ΔM as well as of the $M_{\text{miss}}(D_{\text{tag}}KX_{\text{frag}}\gamma)$ is the signal photon energy resolution. In former case the smearing of the D_s momentum cancels almost completely in the mass difference while in the latter case the impact of experimental smearing of $p_{\text{miss}}(D_{\text{tag}}KX_{\text{frag}})$ on $M_{\text{miss}}(D_{\text{tag}}KX_{\text{frag}}\gamma)$ is minimized by performing the mass constrained vertex of $D_{\text{tag}}KX_{\text{frag}}$ candidates to the nominal D_s^* mass. According to simulated sample the resolutions of ΔM and $M_{\text{miss}}(D_{\text{tag}}KX_{\text{frag}}\gamma)$ are same to within few percent which justifies calibration of $M_{\text{miss}}(D_{\text{tag}}KX_{\text{frag}}\gamma)$ resolution by comparing ΔM resolutions of exclusively reconstructed $D_s^* \rightarrow D_s\gamma$ decays obtained on real data and MC.

In order to calibrate $M_{\text{miss}}(D_{\text{tag}}KX_{\text{frag}}\gamma)$ resolution a fit to the real data ΔM distribution is performed which is described as the sum of signal and background components:

$$\mathcal{F}^{\text{excl}}(\Delta M) = N_{\text{sig}}\mathcal{H}_{\text{sig}}(\Delta M) \otimes \mathcal{G}(\sigma_{\text{cal}}) + N_{\text{bkg}}(1 + c_1\Delta M + c_2\Delta M^2). \quad (6)$$

The signal contribution, $\mathcal{H}_{\text{sig}}(\Delta M) \otimes \mathcal{G}(\sigma_{\text{cal}})$, is parametrized using the histogram PDF obtained on simulated sample, $\mathcal{H}_{\text{sig}}(\Delta M)$, and is numerically convolved with a Gaussian function, $\mathcal{G}(\sigma_{\text{cal}})$. The background is parametrized as the 2nd order polynomial. Best agreement between real data and simulated ΔM distributions are obtained when $\sigma_{\text{cal}} = 2.0 \pm 0.2$ MeV.

The $M_{\text{miss}}(D_{\text{tag}}KX_{\text{frag}}\gamma)$ distributions for each X_{frag} mode of real data inclusive D_s sample with fit results superimposed (see Eq. 5) are shown in Fig. 1. Total inclusive D_s yield on real data sample corresponding to 913 fb^{-1} is found to be 94400 ± 1300 , where uncertainty is statistical only. The PDFs describes well the observed data distributions – the normalized χ^2 values of the fits are between 1.06 and 1.32. Fit residuals exhibit no structures. To estimate the systematic uncertainty on the inclusive D_s yield the fits are repeated by taking $\sigma_{\text{cal}} = 1.8$ or 2.2 MeV.

The inclusive D_s yield, including systematics uncertainties, is found to be

$$N_{D_s}^{\text{inc}} = 94400 \pm 1300(\text{stat.}) \pm 1400(\text{syst.}). \quad (7)$$

We keep only inclusive D_s candidates within the signal window of the $M_{\text{miss}}(D_{\text{tag}}KX_{\text{frag}}\gamma)$, defined as $1.95 < M_{\text{miss}}(D_{\text{tag}}KX_{\text{frag}}\gamma) < 1.99$ GeV, in rest of the analysis, except in case of exclusive reconstruction of $D_s \rightarrow K^-K^+\pi^+$ decays.

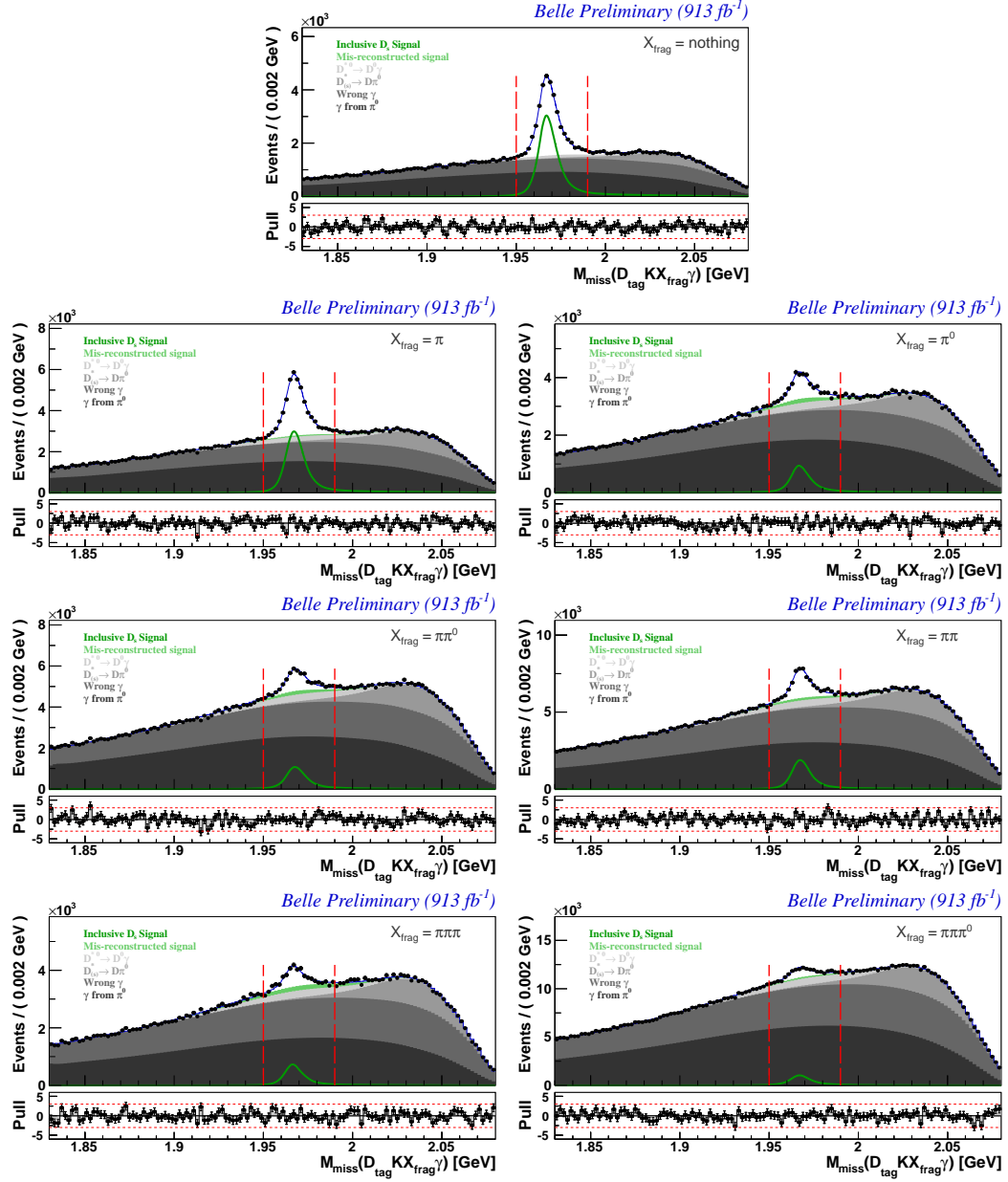


Figure 1: The $M_{\text{miss}}(D_{\text{tag}} K X_{\text{frag}} \gamma)$ distributions for all seven X_{frag} modes with fit results superimposed (solid blue line). Signal contribution is shown with the solid green line, while the full histograms (in different shades of gray) show the contributions of different types of background described in more details in text. The two dashed vertical lines indicate the signal region.

5 Reconstruction of $D_s \rightarrow f$ decays and extraction of absolute $\mathcal{B}(D_s \rightarrow f)$

After reconstructing the inclusive sample of D_s mesons we proceed with the reconstruction of D_s mesons decaying to:

- $D_s^+ \rightarrow K^- K^+ \pi^+$,
- $D_s^+ \rightarrow \bar{K}^0 K^+$,
- $D_s^+ \rightarrow \eta \pi^+$,
- $D_s^+ \rightarrow \mu^+ \nu_\mu$,
- $D_s^+ \rightarrow \tau^+ \nu_\tau$; $\tau^+ \rightarrow e^+ \nu_e \bar{\nu}_\tau$, $\mu^+ \nu_\mu \bar{\nu}_\tau$, $\pi^+ \bar{\nu}_\tau$.

In the following subsections we briefly describe the reconstruction procedure and signal yield extraction for all five studied decay modes, which then enters the calculation of absolute $\mathcal{B}(D_s \rightarrow f)$ as:

$$\mathcal{B}(D_s \rightarrow f) = \frac{N(D_s \rightarrow f)}{N_{D_s}^{\text{inc}} \cdot f_{\text{bias}} \cdot \varepsilon(D_s \rightarrow f | \text{incl. } D_s)}. \quad (8)$$

Above, $N_{D_s}^{\text{inc}}$ is the number of inclusively reconstructed D_s mesons, $N(D_s \rightarrow f)$ is the number of reconstructed $D_s \rightarrow f$ decays within the inclusive D_s sample, and $\varepsilon(D_s \rightarrow f | \text{incl. } D_s)$ is the efficiency of reconstructing $D_s \rightarrow f$ decay within the inclusive D_s sample. We observed on simulated samples that the efficiency of inclusive reconstruction of D_s mesons depends on the D_s decay mode and therefore the inclusively reconstructed D_s sample does not represent truly inclusive sample of D_s mesons. The efficiency drops with increasing multiplicity of final state particles, e.g. $N_{\text{ch}} + N_{\pi^0}$ (where N_{ch} represents the number of charged particles and N_{π^0} the number of neutral pions), produced in D_s decays. In order to take this effect into account a ratio of efficiencies to reconstruct D_s meson inclusively if it decayed to final state f , $\varepsilon_{D_s \rightarrow f}^{\text{inc}}$, and the average efficiency of inclusive D_s reconstruction, $\bar{\varepsilon}_{D_s}^{\text{inc}} = \sum_i \mathcal{B}(D_s \rightarrow i) \varepsilon_{D_s \rightarrow i}^{\text{inc}}$ is included into the denominator of Eq. 8: $f_{\text{bias}} = \varepsilon_{D_s \rightarrow f}^{\text{inc}} / \bar{\varepsilon}_{D_s}^{\text{inc}}$. Ratio f_{bias} is taken from the simulated sample including all known D_s decay modes.

Possible differences between simulated and real data samples in terms of D_s decay modes and their \mathcal{B} s used in our simulation are estimated by studying the distributions of number of particles, $N_{\text{ch}} + N_{\pi^0}$, produced in D_s decays. This distribution on real data is obtained in the following way: first for each inclusive D_s candidate the number of remaining charged tracks, $N_{\text{ch}}^{\text{reco}}$, and π^0 candidates, $N_{\pi^0}^{\text{reco}}$, not associated to $D_{\text{tag}} K X_{\text{frag}} \gamma$ candidate are counted; second fits to the $M_{\text{miss}}(D_{\text{tag}} K X_{\text{frag}} \gamma)$ distributions are performed in bins of $N_{\text{ch}}^{\text{reco}} + N_{\pi^0}^{\text{reco}}$ and the inclusive D_s signal yield

is recorded. The distribution of $N_{\text{ch}}^{\text{reco}} + N_{\pi^0}^{\text{reco}}$ is roughly proportional to the true distribution of $N_{\text{ch}} + N_{\pi^0}$, but with a considerable amount of convolution[§]. The unfolded $N_{\text{ch}} + N_{\pi^0}$ distributions are obtained from $N_{\text{ch}}^{\text{reco}} + N_{\pi^0}^{\text{reco}}$ distribution using the singular value decomposition algorithm. From the distributions of $N_{\text{ch}} + N_{\pi^0}$ obtained on real data and simulated samples and the dependence of inclusive D_s reconstruction efficiency obtained on simulated sample we estimate the the ratio between real data and simulated average inclusive D_s reconstruction efficiencies to be: $\bar{\varepsilon}_{D_s}^{\text{inc}}|_{\text{DATA}}/\bar{\varepsilon}_{D_s}^{\text{inc}}|_{\text{MC}} = 0.9768 \pm 0.0134$. The ratio is consistent with unity within the uncertainty. Nevertheless the inverse of the f_{bias} factor is corrected by the above ratio and its error is taken as a source of systematic uncertainty of measured absolute branching fractions.

5.1 $D_s^+ \rightarrow K^- K^+ \pi^+$

The reconstruction of $D_s^+ \rightarrow K^- K^+ \pi^+$ decays is performed by requiring exactly three charged tracks in the rest of the event with a net charge equal to the charge of inclusively reconstructed D_s candidate. The track with opposite charge to the inclusive D_s^+ candidate is selected to be K^- candidate while the two same-sign tracks are identified as K^+ or π^+ based on their likelihood ratios, $\mathcal{L}_{K,\pi}$.

The exclusively reconstructed $D_s^+ \rightarrow K^- K^+ \pi^+$ candidates are identified as a peak at the nominal mass of the D_s^{*+} in the invariant mass distribution of $K^+ K^- \pi^+ \gamma$ combination, $M(K^+ K^- \pi^+ \gamma)$. Here the γ stands for the signal photon candidate used to reconstruct $D_{\text{tag}} K X_{\text{frag}} \gamma$ candidate. The $M(K^+ K^- \pi^+ \gamma)$ is chosen over $M(K^+ K^- \pi^+)$, because both sides (inclusive and exclusive) have to be correctly reconstructed to produce peaks in $M(K^+ K^- \pi^+ \gamma)$ and $M_{\text{miss}}(D_{\text{tag}} K X_{\text{frag}} \gamma)$. Correctly reconstructed $D_s^+ \rightarrow K^- K^+ \pi^+$ events will namely peak in $M(K^+ K^- \pi^+)$ even if the inclusive reconstruction of D_s candidates failed, e.g. the photon candidate which does not originate from $D_s^* \rightarrow D_s \gamma$ decay is picked up. Since $M(K^- K^+ \pi^+ \gamma)$ and $M_{\text{miss}}(D_{\text{tag}} K X_{\text{frag}} \gamma)$ are correlated due to their common input – γ 4-momentum – no additional selection is applied to the $M_{\text{miss}}(D_{\text{tag}} K X_{\text{frag}} \gamma)$.

The signal yield of exclusively reconstructed $D_s \rightarrow K K \pi$ decays is extracted by fitting the $M(K^+ K^- \pi^+ \gamma)$ distribution. The components of the fit are divided into three categories: correctly reconstructed $D_s^* \rightarrow D_s \gamma \rightarrow K K \pi \gamma$ decays (signal); misreconstructed $D_s^* \rightarrow D_s \pi^0 \rightarrow K^+ K^- \pi^+ \gamma \gamma$ decays, where one of the photons from the π^0 decay is not reconstructed ($D_s^* \rightarrow D_s \pi^0 \rightarrow K K \pi \gamma \gamma$); and random combinations of charged tracks and photons (combinatorial background). The $M(K^+ K^- \pi^+ \gamma)$ distribution is parameterized as:

$$\mathcal{F}(M(K^+ K^- \pi^+ \gamma)) = N_{\text{sig}} \cdot \mathcal{H}_{\text{sig}}(M(K^+ K^- \pi^+ \gamma)) \otimes \mathcal{G}(\sigma_{\text{cal}}^{\text{excl}})$$

[§]E.g. D_s daughter particle might not be reconstructed or a fake charged track or π^0 candidate is counted.

$$\begin{aligned}
& + N_{D_s^* \pi^0} \cdot \mathcal{H}_{D_s^* \pi^0}(M(K^+ K^- \pi^+ \gamma)) \\
& + N_{\text{comb}} \cdot (1 + c_1 \cdot M(K^+ K^- \pi^+ \gamma) + \\
& c_2 \cdot M(K^+ K^- \pi^+ \gamma)^2 + c_3 \cdot M(K^+ K^- \pi^+ \gamma)^3), \quad (9)
\end{aligned}$$

where the signal and $D_s^* \rightarrow D_s \pi^0$ background are parametrized using the non-parametric histogram PDF obtained on a simulated sample (\mathcal{H}), and the combinatorial background is parametrized as a third order polynomial. The signal distribution is convolved with a Gaussian function, $\mathcal{G}(\sigma_{\text{cal}}^{\text{excl}})$, in order to take into account the differences between the resolutions of $M(K^+ K^- \pi^+ \gamma)$ on real data and simulated samples. The $\sigma_{\text{cal}}^{\text{excl}}$ is estimated using the same procedure as described in section 4.1. The only difference is that the resolution on $M(K K \pi \gamma)$ is calibrated instead of the D_s^* and D_s mass difference. We determine $\sigma_{\text{cal}}^{\text{excl}} = 3.2 \pm 0.2$ MeV. Free parameters of the fit are the normalization parameters, N_i , and combinatorial background shape parameters, c_i .

The $M(K^+ K^- \pi^+ \gamma)$ distribution of exclusively reconstructed $D_s \rightarrow K K \pi$ decays within the inclusive D_s sample obtained on real data sample is shown in Fig. 2 with fit results superimposed. The number of correctly reconstructed $D_s \rightarrow K K \pi$ decays is found to be

$$N(D_s \rightarrow K K \pi) = 4094 \pm 123, \quad (10)$$

where the error is statistical only.

5.2 $D_s^+ \rightarrow \bar{K}^0 K^+$

The $D_s^+ \rightarrow \bar{K}^0 K^+$ decays are reconstructed partially by requiring only one additional charged track to be present in rest of the event. The charged track is required to be consistent with kaon hypothesis and has charge equal to that of the inclusively reconstructed D_s candidate. The neutral kaon is not reconstructed at all and it is identified as a peak at the nominal mass of neutral kaon squared in the missing mass squared distribution:

$$M_{\text{miss}}^2(D_{\text{tag}} K X_{\text{frag}} \gamma K) = p_{\text{miss}}^2(D_{\text{tag}} K X_{\text{frag}} \gamma K),$$

where the missing 4-momentum is given by

$$p_{\text{miss}}(D_{\text{tag}} K X_{\text{frag}} \gamma K) = p_{e^+} + p_{e^-} - p_{D_{\text{tag}}} - p_K - p_{X_{\text{frag}}} - p_\gamma - p_K.$$

An explicit reconstruction of \bar{K}^0 meson (via the experimentally accessible $K_S^0 \rightarrow \pi^+ \pi^-$ decays) would lead to a significant signal loss (2/3 of the signal would be lost, without even taking into account the K_S^0 reconstruction efficiency). The signal peak of $D_s^+ \rightarrow \bar{K}^0 K^+$ in $M_{\text{miss}}^2(D_{\text{tag}} K X_{\text{frag}} \gamma K)$ distribution is in addition used to study the differences between M_{miss}^2 resolutions in simulated and real data samples, which

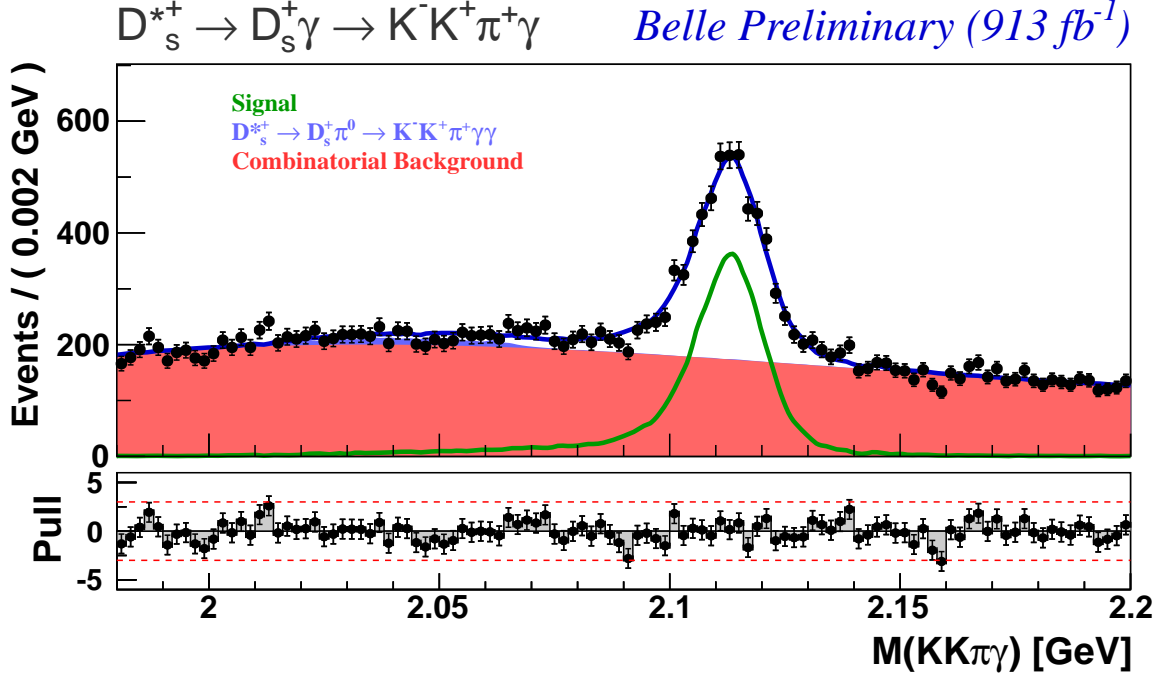


Figure 2: The $M(K^+ K^- \pi^+ \gamma)$ distribution of exclusively reconstructed $D_s \rightarrow K K \pi$ decays within the inclusive D_s sample with fit results superimposed (solid blue line). Solid green line shows the signal contribution, while the full histograms show the contribution of combinatorial background (in red) and $D_s \rightarrow K K \pi$ decays originating from $D_s^* \rightarrow D_s \pi^0$ decay (in blue).

is important in the extraction of yield of $D_s^+ \rightarrow \mu^+ \nu_\mu$ decays. Since the flavor of the neutral kaon is not determined, the doubly Cabibbo suppressed decays, $D_s^+ \rightarrow K^0 K^+$, also contribute to the peak in $M_{\text{miss}}^2(D_{\text{tag}} K X_{\text{frag}} \gamma K)$. Their relative contribution can naively be estimated to be equal to $\tan^4 \theta_C \approx 0.29\%$ (θ_C being the Cabibbo mixing angle), which is order of magnitude below the expected statistical uncertainty and can thus be safely neglected.

The signal yield of partially reconstructed $D_s^+ \rightarrow \bar{K}^0 K^+$ decays is extracted by performing a fit to the $M_{\text{miss}}^2(D_{\text{tag}} K X_{\text{frag}} \gamma K)$ distribution. The candidates are divided into six categories: K^+ candidate originates from the $D_s^+ \rightarrow \bar{K}^0 K^+$ decay and the inclusive D_s candidate is correctly reconstructed (signal); K^+ candidate originates from the $D_s^+ \rightarrow \eta K^+$ decay and the inclusive D_s candidate is correctly reconstructed ($D_s \rightarrow \eta K$ decays); K^+ candidate originates from the $D_s^+ \rightarrow \pi^0 K^+$ decay and the inclusive D_s candidate is correctly reconstructed ($D_s \rightarrow \pi^0 K$ decays); K^+ candidate is mis-reconstructed pion originating from the $D_s^+ \rightarrow \eta \pi^+$ decay and the inclusive D_s candidate is correctly reconstructed ($D_s^+ \rightarrow \eta \pi^+$); K^+ candidate originates from the $D_s \rightarrow K^{*+} \bar{K}^0 \rightarrow K^+ \pi^0 \bar{K}^0$ decay and the inclusive D_s candidate is correctly

reconstructed ($D_s \rightarrow K^{*+} \bar{K}^0$ decays); and all other candidates (combinatorial background). The $M_{\text{miss}}^2(D_{\text{tag}} K X_{\text{frag}} \gamma K)$ distribution is parameterized as:

$$\begin{aligned}
\mathcal{F}(M_{\text{miss}}^2) = & N_{\text{sig}} \cdot \sum_{i=1}^3 \mathcal{G}(M_{\text{miss}}^2, m_{K^0}^2, s_i \sigma_i^{MC}) \\
& + N_{\eta K} \sum_{i=1}^3 \mathcal{G}(M_{\text{miss}}^2, m_{\eta}^2, \sigma_i^{MC}) + N_{\pi^0 K} \sum_{i=1}^3 \mathcal{G}(M_{\text{miss}}^2, m_{\pi^0}^2, \sigma_i^{MC}) \\
& + N_{\eta\pi} [\mathcal{G}(M_{\text{miss}}^2, m_0^{\eta\pi}, \sigma_G) + \mathcal{BG}(M_{\text{miss}}^2, m_0^{\eta\pi}, \sigma_{BG}^{\text{left}}, \sigma_{BG}^{\text{right}})] \\
& + N_{K^* K^0} [\mathcal{G}(M_{\text{miss}}^2, m_0^{K^* K^0}, \sigma_G) + \mathcal{BG}(M_{\text{miss}}^2, m_0^{K^* K^0}, \sigma_{BG}^{\text{left}}, \sigma_{BG}^{\text{right}})] \\
& + N_{\text{comb}} \cdot (1 + c_1 M_{\text{miss}}^2 + c_2 M_{\text{miss}}^2 + c_3 M_{\text{miss}}^3 + c_4 M_{\text{miss}}^4), \quad (11)
\end{aligned}$$

where the signal, and the two peaking backgrounds ($D_s \rightarrow \eta K$ and $D_s \rightarrow \pi^0 K$) are parametrized using the sum of 3 Gaussian functions. All the parameters of the latter peaking backgrounds are fixed to values determined on the simulated sample. In case of the signal all the shape parameters are fixed to the values determined on simulated sample, except the mean ($m_{K^0}^2$) and the common resolution scaling factor of the core and the second Gaussian ($s_1 = s_2 = s$). The width of the third Gaussian (describing the outliers) is fixed. The $\eta\pi$ and $K^* K^0$ candidates are parametrized with a sum of Gaussian and a Bifurcated Gaussian function, where all parameters are fixed to the values determined on simulated sample. The combinatorial background is parametrized with a polynomial of the 4th order, where the coefficients c_i are determined with the fit to the $M_{\text{miss}}^2(D_{\text{tag}} K X_{\text{frag}} \gamma K)$ distribution for candidates in the $M_{\text{miss}}(D_{\text{tag}} K X_{\text{frag}} \gamma) < 1.95$ GeV sideband region. Yields of all event categories are free parameters of the fit, except for the $D_s \rightarrow \eta K$ and $D_s \rightarrow \eta\pi$, which are constrained to expected values based on their known \mathcal{B} s and MC determined efficiencies.

The $M_{\text{miss}}^2(D_{\text{tag}} K X_{\text{frag}} \gamma K)$ distribution of partially reconstructed $D_s^+ \rightarrow \bar{K}^0 K^+$ decays within the inclusive D_s sample obtained on real data sample is shown in Fig. 3 with fit results superimposed. The number of correctly reconstructed $D_s^+ \rightarrow \bar{K}^0 K^+$ decays is found to be

$$N(D_s \rightarrow K^0 K) = 1943 \pm 82, \quad (12)$$

where the error is statistical only.

5.3 $D_s^+ \rightarrow \eta\pi^+$

As in case of $D_s^+ \rightarrow \bar{K}^0 K^+$ decays we perform partial reconstruction of $D_s^+ \rightarrow \eta\pi^+$ decays as well. We require only one charged track consistent with the pion hypothesis to be present in rest of the event. We do not perform any explicit reconstruction of η mesons which are identified as a peak at the nominal mass squared of η in the missing mass squared distribution:

$$M_{\text{miss}}^2(D_{\text{tag}} K X_{\text{frag}} \gamma \pi) = p_{\text{miss}}^2(D_{\text{tag}} K X_{\text{frag}} \gamma \pi),$$

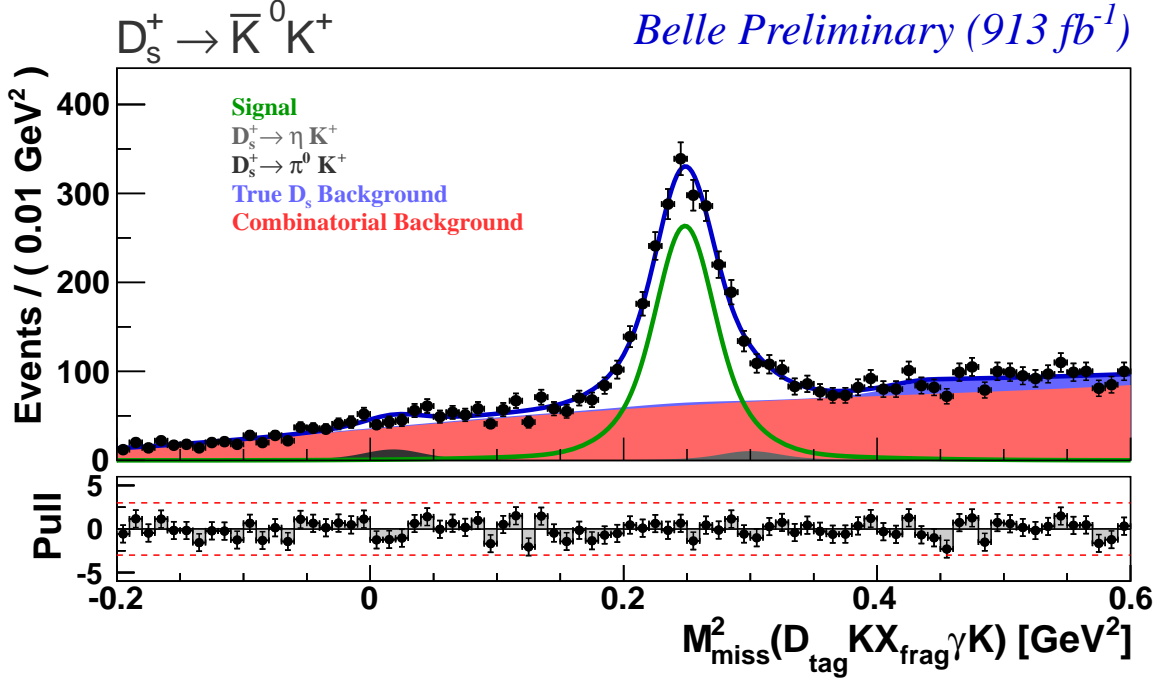


Figure 3: The $M^2_{\text{miss}}(D_{\text{tag}} K X_{\text{frag}} \gamma K)$ distribution of partially reconstructed $D_s^+ \rightarrow \bar{K}^0 K^+$ decays within the inclusive D_s sample with fit results superimposed (solid blue line). Solid green line shows the signal contribution, while the full histograms show the contribution of combinatorial background (in red), $D_s^+ \rightarrow \pi^0 K^+$ (dark gray), $D_s^+ \rightarrow \eta K^+$ (light gray) or other D_s^+ decays (blue).

where the missing 4-momentum is given by

$$p_{\text{miss}}(D_{\text{tag}} K X_{\text{frag}} \gamma \pi) = p_{e^+} + p_{e^-} - p_{D_{\text{tag}}} - p_K - p_{X_{\text{frag}}} - p_\gamma - p_\pi.$$

An explicit reconstruction of η meson would lead to a significant signal loss.

In this sample of inclusive D_s candidate plus additional charged pion there is a significant contribution from $D_s \rightarrow \tau \nu$ decays, when τ lepton decays hadronically to charged pion and neutrino. These events are suppressed by requiring that the extra neutral energy in the ECL (E_{ECL}) to be larger than 1.0 GeV, where the E_{ECL} represents a sum over all energy deposits in the ECL which are not associated to the tracks or neutrals used in inclusive reconstruction of D_s candidates nor the charged pion candidate [21]. The $D_s \rightarrow \tau \nu \rightarrow \pi \nu \nu$ decays namely peak in E_{ECL} at 0, while $D_s \rightarrow \eta \pi$ decays deposit significant amount of energy in the ECL via the η decay products (see section 5.5 for more details).

The signal yield of partially reconstructed $D_s^+ \rightarrow \eta \pi^+$ decays is extracted by performing a fit to the $M^2_{\text{miss}}(D_{\text{tag}} K X_{\text{frag}} \gamma \pi)$ distribution. The candidates are divided into five categories: π^+ candidate originates from the $D_s^+ \rightarrow \eta \pi^+$ decay and the

inclusive D_s candidate is correctly reconstructed (signal); π^+ candidate originates from the $D_s^+ \rightarrow K^0\pi^+$ decay and the inclusive D_s candidate is correctly reconstructed ($D_s \rightarrow K^0\pi$ decays); π^+ candidate is mis-reconstructed kaon originating from the $D_s^+ \rightarrow \bar{K}^0 K^+$ decay and the inclusive D_s candidate is correctly reconstructed ($D_s \rightarrow \bar{K}^0 K$ decays); π^+ candidate originates from the $D_s \rightarrow \rho^0 K^+ \rightarrow \pi^+\pi^- K^+$ decay and the inclusive D_s candidate is correctly reconstructed ($D_s \rightarrow \rho^0 K^+$ decays); and all other candidates (combinatorial background). The $M_{\text{miss}}^2(D_{\text{tag}} K X_{\text{frag}} \gamma \pi)$ distribution is parameterized as:

$$\begin{aligned} \mathcal{F}(M_{\text{miss}}^2) = & N_{\text{sig}} \cdot \sum_{i=1}^3 \mathcal{G}(M_{\text{miss}}^2, m_\eta^2, s_i \sigma_i^{MC}) + N_{K^0\pi} \sum_{i=1}^3 \mathcal{G}(M_{\text{miss}}^2, m_{K^0}^2, \sigma_i^{MC}) \\ & + N_{K^0K} [\mathcal{BG}(M_{\text{miss}}^2, m_0^{K^0K}, \sigma_{BG}^{\text{left}}, \sigma_{BG}^{\text{right}})] + N_{\rho K} [\mathcal{BG}(M_{\text{miss}}^2, m_0^{\rho K}, \sigma_{BG}^{\text{left}}, \sigma_{BG}^{\text{right}})] \\ & + N_{\text{comb}} \cdot (1 + c_1 M_{\text{miss}}^2 + c_2 M_{\text{miss}}^2 + c_3 M_{\text{miss}}^3 + c_4 M_{\text{miss}}^4), \end{aligned} \quad (13)$$

where the signal and the peaking background from $D_s \rightarrow K^0\pi$ decays are parametrized using the sum of three Gaussian functions. All the parameters of the latter peaking background are fixed to values determined on simulated sample. In case of the signal all the shape parameters are fixed, except the mean (m_η^2). The common resolution scaling factor of the core and the second Gaussian ($s_1 = s_2 = s$) is constrained to the value obtained from the fit to the $D_s \rightarrow K^0 K$ sample. The width of the third Gaussian (describing the outliers) is fixed. The $K^0 K$ and ρK candidates are parametrized with a Bifurcated Gaussian function, where all parameters are fixed to the values determined on simulated sample. The combinatorial background is parametrized with a polynomial of the 4th order, where the coefficients c_i are determined with the fit to the $M_{\text{miss}}^2(D_{\text{tag}} K X_{\text{frag}} \gamma \pi)$ distribution for candidates in the $M_{\text{miss}}(D_{\text{tag}} K X_{\text{frag}} \gamma) < 1.95$ GeV sideband region. Yields of all event categories are free parameters of the fit, except for the $K^0\pi$ and $K^0 K$, which are constrained to expected values based on their known \mathcal{B} s and efficiencies determined on simulated sample.

The $M_{\text{miss}}^2(D_{\text{tag}} K X_{\text{frag}} \gamma \pi)$ distribution of exclusively reconstructed $D_s^+ \rightarrow \eta\pi^+$ decays within the inclusive D_s sample obtained on real data sample is shown in Fig. 4 with fit results superimposed. The number of correctly reconstructed $D_s^+ \rightarrow \eta\pi^+$ decays is found to be

$$N(D_s \rightarrow \eta\pi) = 773 \pm 58, \quad (14)$$

where the error is statistical only.

5.4 $D_s^+ \rightarrow \mu^+ \nu_\mu$

The $D_s^+ \rightarrow \mu^+ \nu_\mu$ decays are reconstructed by requiring additional charged track consistent with muon hypothesis to be present in rest of the event. Single missing

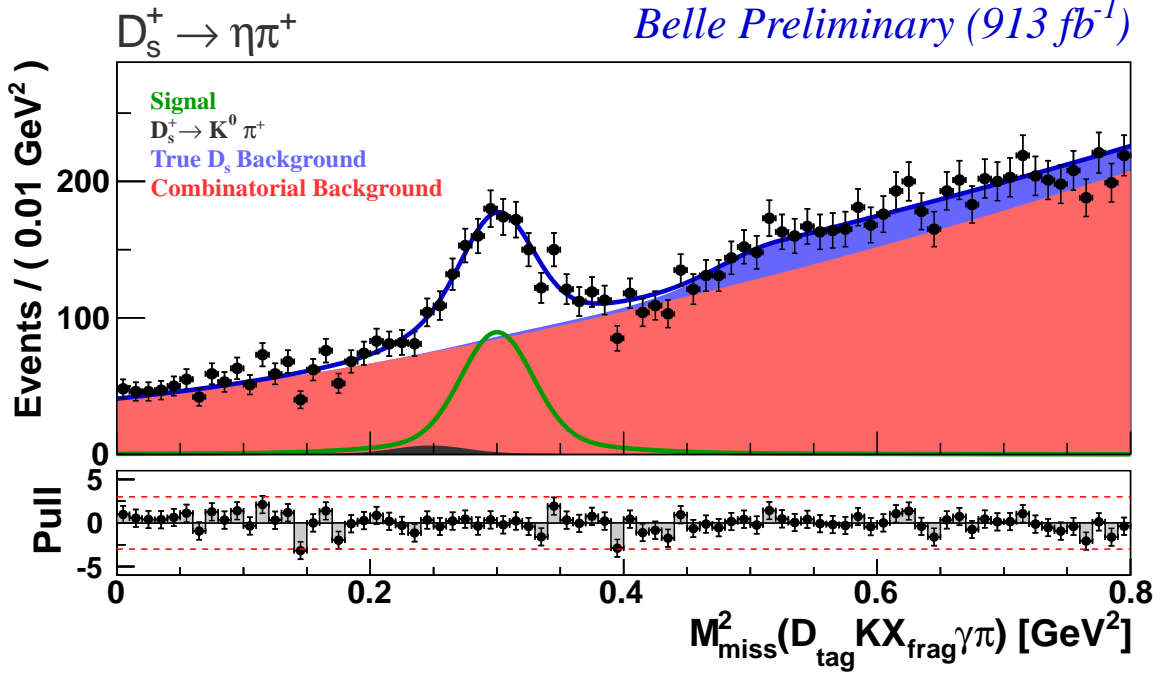


Figure 4: The $M^2_{\text{miss}}(D_{\text{tag}} K X_{\text{frag}} \gamma \pi)$ distribution of partially reconstructed $D_s^+ \rightarrow \eta \pi^+$ decays within the inclusive D_s sample with fit results superimposed (solid blue line). Solid green line shows the signal contribution, while the full histograms show the contribution of combinatorial background (in red), $D_s^+ \rightarrow K^0 \pi^+$ (dark gray), or other D_s^+ decays (blue).

neutrino is then identified as a peak at zero in the missing mass squared distribution:

$$M^2_{\text{miss}}(D_{\text{tag}} K X_{\text{frag}} \gamma \mu) = p^2_{\text{miss}}(D_{\text{tag}} K X_{\text{frag}} \gamma \mu),$$

where the missing 4-momentum is given by

$$p_{\text{miss}}(D_{\text{tag}} K X_{\text{frag}} \gamma \mu) = p_{e^+} + p_{e^-} - p_{D_{\text{tag}}} - p_K - p_{X_{\text{frag}}} - p_\gamma - p_\mu.$$

The signal yield is extracted by performing a fit to the $M^2_{\text{miss}}(D_{\text{tag}} K X_{\text{frag}} \gamma \mu)$ distribution. The candidates are grouped into five categories: μ^+ candidate originates from the $D_s^+ \rightarrow \mu^+ \nu_\mu$ decay and the inclusive D_s candidate is correctly reconstructed (signal); μ^+ candidate is mis-reconstructed kaon originating from the $D_s^+ \rightarrow \bar{K}^0 K^+$ decay and the inclusive D_s candidate is correctly reconstructed ($D_s \rightarrow K^0 K$ decays); μ^+ candidate is mis-reconstructed pion originating from the $D_s^+ \rightarrow \eta \pi^+$ decay and the inclusive D_s candidate is correctly reconstructed ($D_s \rightarrow \eta \pi$ decays); μ^+ candidate originates from the $D_s \rightarrow \tau \nu_\tau \rightarrow \mu \nu_\tau \nu_\mu$ decay and the inclusive D_s candidate

is correctly reconstructed ($D_s \rightarrow \tau \nu_\tau$); and all other candidates (combinatorial background). The $M_{\text{miss}}^2(D_{\text{tag}} K X_{\text{frag}} \gamma \mu)$ distributions is parameterized as:

$$\begin{aligned} \mathcal{F}(M_{\text{miss}}^2) = & N_{\text{sig}} \cdot \sum_{i=1}^3 \mathcal{G}(M_{\text{miss}}^2, m_0^2, s_i \sigma_i^{MC}) + N_{\eta\pi} \sum_{i=1}^2 \mathcal{G}(M_{\text{miss}}^2, m_\eta^2, \sigma_i^{MC}) \\ & + N_{K^0 K} \mathcal{BG}(M_{\text{miss}}^2, m_0^{K^0 K}, \sigma_{BG}^{\text{left}}, \sigma_{BG}^{\text{right}}) \\ & + N_\tau \text{Exp}(t_\tau) + N_{\text{comb}} \text{Exp}(t_{\text{comb}}), \end{aligned} \quad (15)$$

where the signal and the peaking background $D_s \rightarrow \eta\pi$ are parametrized using the sum of 3 and 2 Gaussian functions, respectively. All the parameters of the latter peaking background are fixed to values determined on MC sample. In case of the signal all the shape parameters are fixed, except the mean (m_0^2). The common resolution scaling factor of the core and the second Gaussian ($s_1 = s_2 = s$) is constrained (not fixed) to the value obtained on the $D_s \rightarrow K^0 K$ and $D_s \rightarrow \eta\pi$ samples. The width of the third Gaussian (describing the outliers) is fixed. The $K^0 K$ candidates are parametrized with a Bifurcated Gaussian function, where all parameters are fixed to the values determined on MC sample. The $D_s \rightarrow \tau \nu_\tau$ and combinatorial backgrounds are parametrized with a exponential function, where the shape parameter of the combinatorial background is determined with the fit to the $M_{\text{miss}}^2(D_{\text{tag}} K X_{\text{frag}} \gamma \mu)$ distribution for candidates in the $M_{\text{miss}}(D_{\text{tag}} K X_{\text{frag}} \gamma) < 1.95$ GeV sideband region and it is fixed to MC determined value for $\tau \nu_\tau$ decays. Yields of all event categories are free parameters of the fit, except for the $\eta\pi$ and $K^0 K$, which are constrained to expected values based on their known \mathcal{B} s and MC determined efficiencies. An important peaking background could arise from the $D_s^+ \rightarrow \pi^+ \pi^0$ decays, which would peak near the signal $D_s^+ \rightarrow \mu^+ \nu_\mu$ decays (at $m_{\pi^0}^2 = 0.018$ GeV²). These decays were not observed so far and based on the upper limit of $\mathcal{B}(D_s^+ \rightarrow \pi^+ \pi^0) < 3.4 \times 10^{-4}$ at 90% C.L. set by CLEO-c [22] their contribution is estimated to be less than 1 event. Their contribution is therefore negligible and is not taken into account.

The distribution of $M_{\text{miss}}(D_{\text{tag}} K X_{\text{frag}} \gamma \mu)$ with superimposed fit result is shown in Fig.5. The number of reconstructed $D_s \rightarrow \mu \nu$ decays is found to be

$$N(D_s^+ \rightarrow \mu^+ \nu_\mu) = 489 \pm 26, \quad (16)$$

where the error is statistical only.

5.5 $D_s^+ \rightarrow \tau^+ \nu_\tau$

The reconstruction of $D_s^+ \rightarrow \tau^+ \nu_\tau$ is performed by requiring one charged track to be present in rest of the event and is identified as an electron, muon or a pion (denoted as $D_s \rightarrow \tau(X) \nu$ where $X = e, \mu, \pi$) indicating subsequent decay of τ lepton to $e \nu_e \nu_\tau$, $\mu \nu_\mu \nu_\tau$ or $\pi \nu_\tau$. Due to the multiple neutrinos in the final state these decays do not

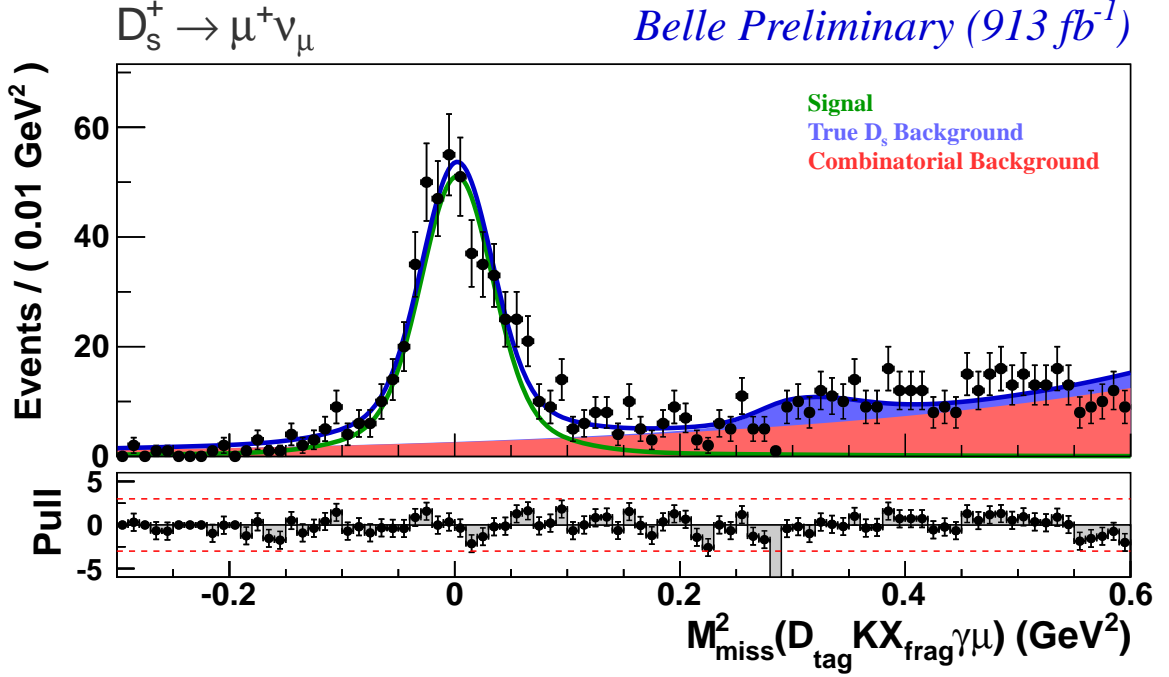


Figure 5: The $M_{\text{miss}}^2(D_{\text{tag}} K X_{\text{frag}} \gamma \mu)$ distribution of exclusively reconstructed $D_s^+ \rightarrow \mu^+ \nu_\mu$ decays within the inclusive D_s sample fit results superimposed (solid blue line). The solid green line shows the contribution of signal, while the contributions of combinatorial background and background other D_s decays are indicated by the shaded red and blue areas, respectively.

peak in the missing mass squared distribution:

$$M_{\text{miss}}^2(D_{\text{tag}} K X_{\text{frag}} \gamma X) = p_{\text{miss}}^2(D_{\text{tag}} K X_{\text{frag}} \gamma X),$$

where the missing 4-momentum is given by

$$p_{\text{miss}}(D_{\text{tag}} K X_{\text{frag}} \gamma X) = p_{e^+} + p_{e^-} - p_{D_{\text{tag}}} - p_K - p_{X_{\text{frag}}} - p_\gamma - p_X.$$

The background in $D_s \rightarrow \tau(\pi)\nu$ sample is much larger than in the leptonic modes which however can be significantly reduced by requiring the missing momentum of the event, $p_{\text{miss}}(D_{\text{tag}} K X_{\text{frag}} \gamma \pi)$, to be larger than 1.2 GeV. Background in this sample can be further reduced by requiring $0.0 < M_{\text{miss}}^2(D_{\text{tag}} K X_{\text{frag}} \gamma \pi) < 0.6 \text{ GeV}^2$ [¶]. In case of $D_s \rightarrow \tau \nu_\tau \rightarrow \ell \nu_\tau \nu_\tau \nu_\ell$ we require $M_{\text{miss}}^2(D_{\text{tag}} K X_{\text{frag}} \gamma \ell) > 0.3 \text{ GeV}^2$ in order to veto contribution of $D_s^+ \rightarrow \ell^+ \nu_\ell$ decays.

[¶]Due to the lack of phase space and the fact that $D_s \rightarrow \tau \nu_\tau \rightarrow \pi \nu_\tau$ decays have only two neutrinos in the final state these decays populate relatively narrow region in $M_{\text{miss}}^2(D_{\text{tag}} K X_{\text{frag}} \gamma \pi)$.

The signal yield of $D_s \rightarrow \tau(X)\nu_\tau$ decays is extracted from the fits to the E_{ECL} distributions. The candidates are divided into three categories: X originates from the $D_s \rightarrow \tau(X)\nu_\tau$ decay and the inclusive D_s candidate is correctly reconstructed (signal); small contribution from other τ decays (cross-feed) is also considered as signal; X originates from a D_s decay such as semileptonic $h\ell\nu$ decays (when $X = \ell$) or hadronic D_s decay modes (when $X = \pi$) and inclusive D_s candidate is correctly reconstructed ($D_s \rightarrow f$ background); and all other candidates (combinatorial background). The E_{ECL} distribution is parametrized as:

$$\begin{aligned} \mathcal{F}(E_{ECL}) = & N_{\tau(X)} \cdot \mathcal{H}_{\tau(X)}(E_{ECL}) \\ & + \sum_f N_{D_s \rightarrow f} \cdot \mathcal{H}_{D_s \rightarrow f}(E_{ECL}) + N_{\text{comb}} \cdot \mathcal{H}_{\text{comb}}(E_{ECL}), \end{aligned} \quad (17)$$

where all components are described with non-parametric histogram PDF (\mathcal{H}) taken from simulated samples.

The distributions of E_{ECL} for $D_s \rightarrow \tau(e)\nu$, $D_s \rightarrow \tau(\mu)\nu$, and $D_s \rightarrow \tau(\pi)\nu$ decays are shown in Fig. 6 with fit results superimposed. The number of reconstructed signal decays are found to be:

$$N(D_s \rightarrow \tau(e)\nu_\tau) = 952 \pm 59, \quad (18)$$

$$N(D_s \rightarrow \tau(\mu)\nu_\tau) = 758 \pm 48 \quad (19)$$

$$N(D_s \rightarrow \tau(\pi)\nu_\tau) = 496 \pm 35, \quad (20)$$

where the errors are statistical only.

6 Results and Systematics

From the extracted signal yields of studied D_s decay modes we determine their absolute branching fractions using Eq. 8. They are summarized in Table 2 and are found to be consistent with previous measurements performed by CLEO and Babar collaborations.

Systematic errors for the measured branching fractions are associated with the uncertainties in the signal yields, the efficiencies, and the number of inclusively reconstructed D_s .

The systematic error^{||} related to the normalization is assigned to be 1.95% (see Eq. 7) and is common for all studied $D_s \rightarrow f$ decays. As described in Sec. 5 the f_{bias} factor is corrected by the $\bar{\epsilon}_{D_s}^{\text{inc.}}|_{\text{DATA}}/\bar{\epsilon}_{D_s}^{\text{inc.}}|_{\text{MC}}$ ratio and the uncertainty on the correction (1.37%) is assigned as systematic error referred to as tag bias and is common for all $D_s \rightarrow f$ decays. The systematic errors in the $D_s \rightarrow f$ reconstruction

^{||}All systematic errors are given as relative uncertainties.

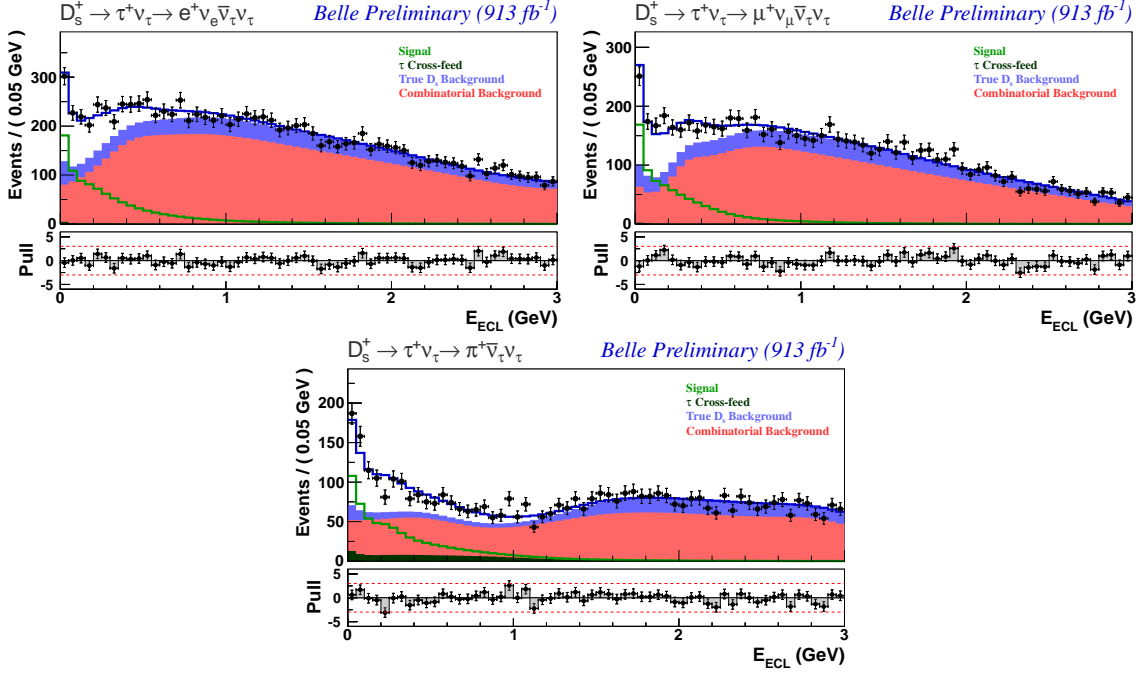


Figure 6: The E_{ECL} distribution of exclusively reconstructed $D_s \rightarrow \tau(e)\nu_\tau$ (top left), $D_s \rightarrow \tau(\mu)\nu_\tau$ (top right), and $D_s \rightarrow \tau(\pi)\nu_\tau$ (bottom) decays within the inclusive D_s sample with fit results superimposed. The solid green lines show the contribution of signal and the contribution of τ cross-feeds are indicated by the full dark green histograms. The contributions of combinatorial background and background from other $D_s \rightarrow f$ decays is indicated by the shaded red and blue areas, respectively.

efficiencies arise from the uncertainty in tracking efficiency (0.35% per reconstructed charged track in the final state of $D_s \rightarrow f$ decay), particle identification efficiency, branching fractions of τ decays, and MC statistics. All of these depend on the studied $D_s \rightarrow f$ decay. The systematic error from MC statistics of the histogram PDFs is evaluated by varying the content of each bin by its statistical uncertainty in case of $D_s \rightarrow \tau\nu_\tau$ signal yields. The shape parameters of combinatorial background are varied within their uncertainties and the differences with respect to the nominal fits are taken as the systematic uncertainty in case of $D_s^+ \rightarrow \mu^+\nu_\mu$, $D_s \rightarrow K^0K^+$, and $D_s \rightarrow \eta\pi$ decays. To estimate the systematic error due to the possible signal E_{ECL} shape difference between MC and data, the ratio of data to MC for the background subtracted E_{ECL} histograms of the $D_s \rightarrow KK\pi$ and $D_s \rightarrow K^0K^+$ samples is fitted with a fourth-order polynomial and the signal E_{ECL} PDF is modified within the fitted errors. Similarly we estimate the systematic error due to the possible combinatorial E_{ECL} shape between MC and data by fitting the ratio of E_{ECL} histograms of $D_s \rightarrow \tau\nu_\tau$ candidates populating the $M_{\text{miss}}(D_{\text{tag}}KX_{\text{frag}}\gamma)$ sideband region (defined as

| D_s^+ Decay Mode | Signal Yield | $f_{\text{bias}} \cdot \varepsilon(D_s \rightarrow f \text{incl. } D_s)$ | $\mathcal{B} [\%]$ |
|-------------------------------|----------------|--|---------------------------------|
| $K^- K^+ \pi^+$ | 4094 ± 123 | 0.8578 ± 0.0056 | $5.06 \pm 0.15 \pm 0.19$ |
| $\bar{K}^0 K^+$ | 1943 ± 82 | 0.7254 ± 0.0054 | $2.84 \pm 0.12 \pm 0.08$ |
| $\eta \pi^+$ | 773 ± 58 | 0.4577 ± 0.0064 | $1.79 \pm 0.14 \pm 0.05$ |
| $\mu \nu_\mu$ | 489 ± 26 | 0.9813 ± 0.0175 | $0.528 \pm 0.028 \pm 0.019$ |
| $\tau \nu_\tau$ (e mode) | 952 ± 59 | 1.0531 ± 0.0135 | $5.37 \pm 0.33^{+0.35}_{-0.30}$ |
| $\tau \nu_\tau$ (μ mode) | 758 ± 48 | 0.7849 ± 0.0118 | $5.88 \pm 0.37^{+0.34}_{-0.58}$ |
| $\tau \nu_\tau$ (π mode) | 496 ± 35 | 0.8072 ± 0.0152 | $5.96 \pm 0.42^{+0.45}_{-0.39}$ |
| $\tau \nu_\tau$ (Combined) | | | $5.70 \pm 0.21^{+0.31}_{-0.30}$ |

Table 2: Signal yields, tag bias corrected efficiencies and measured branching fractions for all five studied D_s^+ decay modes. The first uncertainty is statistical and the second is systematic.

$M_{\text{miss}}(D_{\text{tag}} K X_{\text{frag}} \gamma) < 1.94 \text{ GeV}$ or $M_{\text{miss}}(D_{\text{tag}} K X_{\text{frag}} \gamma) > 2.00 \text{ GeV}$ with a linear function and modifying the combinatorial E_{ECL} PDF within the fit errors. The uncertainties for the branching fractions of D_s decays the true D_s background categories that are fixed in the fits are estimated by changing the branching fractions by their experimental errors [1]. In case of $D_s \rightarrow \tau(e)\nu_\tau$ and $D_s \rightarrow \tau(\mu)\nu_\tau$ decays the largest contribution to the systematic uncertainty originates from $D_s \rightarrow K^0 \ell \nu$ decays and in case of $D_s \rightarrow \tau(\pi)\nu_\tau$ from $D_s \rightarrow \eta \pi$ and ρK decays. The τ cross-feed is fixed relative to the signal contribution in the nominal fit to the E_{ECL} distributions of $D_s \rightarrow \tau \nu$ samples. The ratios are varied within their uncertainties and the fits are repeated and the differences from the nominal fits are taken as the systematic uncertainties.

The total systematic error is calculated by summing the above uncertainties in quadrature. The estimated systematic errors are summarized in Tables 3 and 4 for the hadronic and leptonic D_s decay modes, respectively.

7 Extraction of f_{D_s} and Conclusions

The value of f_{D_s} is determined from measured branching fractions of leptonic D_s decays. Inverting Eq. 1 yields

$$f_{D_s} = \frac{1}{G_F m_\ell \left(1 - \frac{m_\ell^2}{M_{D_s}^2}\right) |V_{cs}|} \sqrt{\frac{8\pi \mathcal{B}(D_s \rightarrow \ell \nu_\ell)}{M_{D_s} \tau_{D_s}}}.$$

The external inputs necessary in the extraction of f_{D_s} from the measured \mathcal{B} s are given in Table 5. The $|V_{cs}|$ is obtained from the very well measured $|V_{ud}| = 0.97425(22)$ and $|V_{cb}| = 0.04$ from an average of exclusive and inclusive semileptonic B decay results

| Source | $K^- K^+ \pi^+$ [%] | $\bar{K}^0 K^+$ [%] | $\eta \pi^+$ [%] |
|-----------------------|---------------------|---------------------|------------------|
| Statistical | 3.00 | 4.22 | 7.50 |
| Normalization | 1.95 | 1.95 | 1.95 |
| Tag bias | 1.37 | 1.37 | 1.37 |
| Tracking | 1.05 | 0.35 | 0.35 |
| Efficiency | 0.65 | 0.74 | 1.40 |
| PID | 2.57 | 0.82 | 1.08 |
| Signal PDF | 0.82 | – | – |
| True D_s background | – | 0.56 | 0.65 |
| Total syst. | 3.81 | 2.71 | 3.06 |
| Stat. + Syst. | 4.85 | 5.02 | 8.10 |

Table 3: Summary of systematic uncertainties for the branching fraction measurement of hadronic D_s decays.

| Source | $\mu\nu$ [%] | $\tau(e)\nu$ [%] | $\tau(\mu)\nu$ [%] | $\tau(\pi)\nu$ [%] | $\tau\nu$ [%] |
|-----------------------------------|--------------|--------------------|--------------------|--------------------|--------------------|
| Statistical | ± 5.32 | ± 6.18 | ± 6.33 | ± 7.04 | ± 3.75 |
| Normalization | ± 1.95 | ± 1.95 | ± 1.95 | ± 1.95 | ± 1.95 |
| Tag bias | ± 1.37 | ± 1.37 | ± 1.37 | ± 1.37 | ± 1.37 |
| Efficiency | ± 1.78 | ± 1.28 | ± 1.51 | ± 1.88 | ± 0.84 |
| Tracking | ± 0.35 | ± 0.35 | ± 0.35 | ± 0.35 | ± 0.35 |
| PID | ± 1.96 | ± 2.03 | ± 1.93 | ± 0.88 | ± 1.70 |
| Signal PDF | – | +3.46 | +1.96 | +3.43 | +2.95 |
| Comb. bkg. PDF | ± 0.02 | +0.11 | –8.31 | +0.92 | –2.54 |
| PDF stat. | – | ± 2.16 | ± 2.19 | ± 3.05 | ± 1.44 |
| True D_s background | ± 0.82 | ± 3.88 | ± 3.56 | ± 3.15 | ± 2.84 |
| τ cross-feed | – | ± 0.36 | ± 0.24 | ± 3.71 | ± 0.94 |
| $\mathcal{B}(\tau \rightarrow X)$ | – | ± 0.22 | ± 0.23 | ± 0.64 | ± 0.19 |
| Total syst. | ± 3.67 | $+6.59$ -5.61 | $+5.76$ -9.92 | $+7.49$ -6.60 | $+5.40$ -5.19 |
| Stat. + Syst. | ± 6.46 | $+9.03$ -8.35 | $+8.56$ -11.8 | $+10.3$ -9.65 | $+6.57$ -6.40 |

Table 4: Summary of systematic uncertainties for the branching fraction measurement of leptonic D_s decays.

as discussed in Ref. [23] by using the following relation:

$$|V_{cs}| = |V_{ud}| - \frac{1}{2}|V_{cb}|^2.$$

| Quantity | Value |
|--------------|---|
| M_{D_s} | 1.96847(33) GeV |
| m_τ | 1.77682(16) GeV |
| m_μ | 0.105658367(9) GeV |
| τ_{D_s} | 0.500(7) ps |
| G_F | $1.16637(1) \times 10^{-5}$ GeV $^{-2}$ |
| $ V_{cs} $ | 0.97345(22) |

Table 5: Numerical values of external parameters used in extraction of f_{D_s} .

| $D_s \rightarrow \ell \nu$ | f_{D_s} [MeV] |
|----------------------------|---|
| $\mu\nu$ | $249.0 \pm 6.6(\text{stat.}) \pm 4.6(\text{syst.}) \pm 1.7(\tau_{D_s})$ |
| $\tau\nu$ | $261.9 \pm 4.9(\text{stat.}) \pm 7.0(\text{syst.}) \pm 1.8(\tau_{D_s})$ |
| Combination | $255.0 \pm 4.2(\text{stat.}) \pm 4.7(\text{syst.}) \pm 1.8(\tau_{D_s})$ |

Table 6: Measured values of f_{D_s} in $\mu\nu$ and $\tau\nu$ decay modes and the combination of the two.

The external inputs are all very precisely measured and do not introduce additional uncertainties except the D_s lifetime, τ_{D_s} , which introduces an 0.70% relative uncertainty on f_{D_s} . Table 6 summarizes the obtained values of f_{D_s} using the $D_s^+ \rightarrow \mu^+ \nu_\mu$ and $D_s^+ \rightarrow \tau^+ \nu_\tau$ decays. An error-weighted average of f_{D_s} is found to be

$$f_{D_s} = (255.0 \pm 4.2(\text{stat.}) \pm 4.7(\text{syst.}) \pm 1.8(\tau_{D_s})) \text{ MeV},$$

where the correlation of the systematic uncertainties between the $\mu\nu$ and $\tau\nu$ have been taken into account. This is the most precise measurement of f_{D_s} up to date.

ACKNOWLEDGEMENTS

We thank the KEKB group for the excellent operation of the accelerator; the KEK cryogenics group for the efficient operation of the solenoid; and the KEK computer group, the National Institute of Informatics, and the PNNL/EMSL computing group for valuable computing and SINET4 network support. We acknowledge support from the Ministry of Education, Culture, Sports, Science, and Technology (MEXT) of Japan, the Japan Society for the Promotion of Science (JSPS), and the Tau-Lepton Physics Research Center of Nagoya University; the Australian Research Council and the Australian Department of Industry, Innovation, Science and Research; the National Natural Science Foundation of China under contract No. 10575109, 10775142, 10875115 and 10825524; the Ministry of Education, Youth and Sports of the Czech

Republic under contract No. LA10033 and MSM0021620859; the Department of Science and Technology of India; the Istituto Nazionale di Fisica Nucleare of Italy; the BK21 and WCU program of the Ministry Education Science and Technology, National Research Foundation of Korea Grant No. 2010-0021174, 2011-0029457, 2012-0008143, 2012R1A1A2008330, BRL program under NRF Grant No. KRF-2011-0020333, and GSDC of the Korea Institute of Science and Technology Information; the Polish Ministry of Science and Higher Education and the National Science Center; the Ministry of Education and Science of the Russian Federation and the Russian Federal Agency for Atomic Energy; the Slovenian Research Agency; the Basque Foundation for Science (IKERBASQUE) and the UPV/EHU under program UFI 11/55; the Swiss National Science Foundation; the National Science Council and the Ministry of Education of Taiwan; and the U.S. Department of Energy and the National Science Foundation. This work is supported by a Grant-in-Aid from MEXT for Science Research in a Priority Area (“New Development of Flavor Physics”), and from JSPS for Creative Scientific Research (“Evolution of Tau-lepton Physics”).

References

- [1] K. Nakamura *et al.* (Particle Data Group), J. Phys. G **37**, 075021 (2010).
- [2] J. L. Rosner and S. Stone, arXiv:1201.2401 [hep-ex].
- [3] J. P. Alexander *et al.* (CLEO Collaboration), Phys. Rev. D **79**, 052001 (2009); M. Artuso *et al.* (CLEO Collaboration), Phys. Rev. Lett. **99**, 071802 (2007).
- [4] P. Naik *et al.* (CLEO Collaboration), Phys. Rev. D **80**, 112004 (2009).
- [5] P. U. E. Onyisi *et al.* (CLEO Collaboration), Phys. Rev. D **79**, 052002 (2009); K. M. Ecklund *et al.* (CLEO Collaboration), Phys. Rev. Lett. **100**, 161801 (2008).
- [6] L. Widhalm *et al.* (Belle Collaboration), Phys. Rev. Lett. **100**, 241801 (2008).
L. Widhalm, Belle Note 997.
- [7] P. del Amo Sanchez *et al.* (BaBar Collaboration), Phys. Rev. D **82**, 091103 (2010) [arXiv:1008.4080].
- [8] C. T. H. Davies *et al.* (HPQCD Collaboration), Phys. Rev. D **82**, 114504 (2010) [arXiv: 1008.4018].
- [9] A. Bazavov *et al.* (Fermilab/MILC Collaboration), [arXiv:1112.3051], submitted to Phys. Rev. D.
- [10] B. Blossier *et al.*, JHEP **0907**, 043 (2009) [arXiv:0904.0954].

- [11] J. Bordes, J. Peñarrocha, and K. Schilcher, JHEP **0511**, 014 (2005).
- [12] W. Lucha, D. Melikhov, and S. Simula, Phys. Lett. B **701**, 82 (2011).
- [13] A. M. Badalian *et al.*, Phys. Rev. D **75**, 116001 (2007); see also A. M. Badalian and B. L. G. Bakker, [hep-ph/0702229].
- [14] C.-W. Hwang, Phys. Rev. D **81**, 054022 (2010) [arXiv:0910.0145].
- [15] A. G. Akeroyd and C. H. Chen, Phys. Rev. D **75**, 075004 (2007).
- [16] S. Kurokawa and E. Kikutani, Nucl. Instr. and Meth. A **499**, 1 (2003), and other papers included in this volume.
- [17] A. Abashian *et al.* (Belle Collab.), Nucl. Instr. and Meth. A **479**, 117 (2002).
- [18] Z. Natkaniec *et al.* (Belle SVD2 Group), Nucl. Instr. and Meth. A **560**, 1 (2006).
- [19] M. Feindt and U. Kerzel, Nucl. Instrum. Meth. A **559**, 190 (2006).
- [20] M. Pivk and F. R. Le Diberder, Nucl. Instrum. Meth. A **555**, 356 (2005) [physics/0402083 [physics.data-an]].
- [21] K. Ikado *et al.* [Belle Collaboration], Phys. Rev. Lett. **97**, 251802 (2006) [hep-ex/0604018].
- [22] H. Mendez *et al.* [CLEO Collaboration], Phys. Rev. D **81**, 052013 (2010) [arXiv:0906.3198 [hep-ex]].
- [23] M. Artuso, E. Barberio and S. Stone, PMC Physics A, 3:3 (2009) [arXiv:0902.3743].